14

Magnetic nanoparticles dynamics modeling in the shell of polyelectrolyte capsules in a low-frequency magnetic field

© I.A. Burmistrov,[1] S.L. Gribanovsky,[2] D.B. Trushina[1]

[1] Institute of Crystallography named after A.V. Shubnikov of Kurchatov Center of Crystallography and Photonics Scientific Research Center
glqq Kurchatov Institute“
119333 Moscow, Russia
[2] Scientific and Educational Center „Nanomaterials and nanotechnologies“
of Tambov State University named after G.R. Derzhavin,
392000 Tambov, Russia
e-mail: burmiivan@gmail.com

Received September 4, 2024
Revised February 24, 2025
Accepted February 26, 2025

Numerical modelling of the rotation of a single-domain magnetic nanoparticle in the shell of a polyelectrolyte capsule under the action of a low-frequency magnetic field has been carried out. Was demonstrated the possibility of resonant increase of the rotation amplitude of magnetic nanoparticles in the studied system. From the modelling results it was determined that pulsed modes of exposure to low frequency magnetic field are more promising for controlled release of encapsulated substances.

Keywords: magnetic nanoparticles, polyelectrolyte capsules, low-frequency magnetic field, shell permeability control, pulsed magnetic field.

DOI: 10.61011/TP.2025.06.61387.268-24

Introduction

The development of targeted drug delivery systems may significantly improve the effectiveness, safety, and convenience of drug administration for patients. Micro- and nano-systems are a promising platform for the targeted drug delivery [1–3].

Polyelectrolyte capsules (PEC) are quite versatile and multifunctional carriers to provide the targeted drug delivery [4,5]. Since PEC shell is highly functional it is possible to create the carriers sensitive to different physical effects, such as temperature [6,7], ultrasound [8], laser radiation [9], magnetic field [10,11]. Sensitization can be used to control the release of a drug from PEC.

The current research focus is shifted: instead of increasing the accumulation of drug carriers in a given area of the body a controlled local release of substances is proposed [2,12]. Control of drug release from carriers plays a key role in improving the effectiveness of therapeutic systems. The inability to precisely adjust the substance release parameters can lead to insufficient concentration of the active substance in the target area or to its excessive release, which may cause toxic effects[13]. Controlled drug release due to external effects allows ensuring a more efficient impact on the therapeutic target by locally maintaining drug concentration in the therapeutic window [14]. Due to modeling the effects of various carrier parameters on the release process we may better understand how these factors can be adjusted to achieve the desired rate and volume of drug release, which is critical for improving the effectiveness and safety of therapy.

1. Release mechanisms

Various mechanisms of substances release from PEC are known. The main mechanisms of substances release from the capsules include diffusion of substances along a concentration gradient, erosion of the shell (washout of polymer from the complex), chemical destruction of the shell (proteolytic cleavage of shell polymers, hydrolysis of polymers, etc.), shell rupture under the action of internal pressure (including osmosis), changes in the phase state of the shell, changes in porosity of the shell [15,16]. These mechanisms may be classified as non-destructive, i.e. when the microcapsule structure stays intact (diffusion, shell porosity change), and destructive ones (erosion, hydrolysis, phase change, release after osmosis). Of particular interest are non-destructive release mechanisms that can be controlled remotely.

1.1. Change of porosity

The change in porosity of the shell for controlled release is based on the temperature sensitivity of polymers. For example, for capsules based on poly(N-isopropylacrylamide) at temperatures below the lower critical temperature of about 32 °C, linear chains swell and cover the pores in the shells, reducing diffusion. As the temperature rises, polymers with different temperature sensitivities can change

their conformation to varying extent. This results in larger sizes of pores in the microcapsule shell. Thus, the shell has better permeability [17]. A change in the temperature of the microcapsule shell can be achieved both by heating the entire volume where the microcapsules are located [18], and by locally heating the shell, for example, using laser radiation [19].

1.2. Diffusion mechanism

The diffusion release mechanism is based on the difference in concentrations of the encapsulated substance between the external environment and the internal volume of microcapsules. The diffusion of substances through the shell depends on the thickness of the shell [20], molecular weight of the encapsulated substance [21,22], rate of diffusion of the encapsulated substance in the environment from the surface of the microcapsule [23], etc.

A controlled remote change in permeability of the microcapsule shell, leading to a change in the diffusion rate, can be achieved by heating [24] or mechanical deformation [6,25].

One of the promising methods for creating mechanical deformations in a local volume is the use of a magnetic field. In this case mechanical deformations occur after the energy of the low-frequency magnetic field (LFMF) is transformed into mechanical rotation of the shell-integrated magnetic nanoparticles (MNP). At that, the direction of magnetic moment of MNP under the action of LFMF changes due to rotation of the particle itself [27]. Such mechanism of interaction between MNP and LFMF is named Brownian relaxation.

1.3. MNP as local mediators of mechanical deformations

An extensive theoretical analysis of MNP rotation behavior when exposed to LFMF to create mechanical deformations is presented in the works of Yu.I. Golovin and co-authors. This paper analyzed the influence of MNP parameters (size of magnetic core, magnetic moment and etc.) and elastic characteristics of macromolecules on the force and magnitude of deformation that occurs in the system MNP−macromolecule−MNP when exposed to LFMF [28]. It has been shown that in systems MNP−macromolecule−MNP located in an aqueous medium, the viscous and elastic forces have no significant effect at LFMF frequencies below $\sim 10^4$ Hz. It is shown that, with the correct selection of system parameters, it is possible to obtain forces applied to a macromolecule sufficient to change the topology of its active centers and secondary/tertiary structure. It is shown that in an alternating magnetic field with an induction of 0.1−1 T and a circular frequency of $\leq 10^4\,\mathrm{s}^{-1}$ in macromolecules, forces up to several hundred pN can be induced and absolute deformation up to several tens of nm can be caused, developing compression and shear stresses up to 10^8 Pa [28–30].

Yu.I. Golovin and co-authors theoretically proved that the use of anisotropic MNP is more promising than the use of spherical MNP, as it allows to achieve stronger deformations with similar parameters of LFMF [31].

In a recent review by Cecile Naud et al. a drastic growth of the number of studies where MNP are used as local mediators of mechanical deformations for cancer therapy is noticed [32]. In a number of papers not included in this review, the possibility of using MNP as local mediators of mechanical deformations has been experimentally demonstrated. It has been shown that the forces achieved are sufficient to modulate the activity of enzyme jcite33, activate the ion channels and disrupt the integrity of the cell membrane jcite34, cause dissociation of complementary chains of the short DNA duplexes jcite35, and induce the death of the tumor-associated fibroblasts by damaging their lysosomes [36], control the cell differentiation and migration in tissues in *in vivo* conditions [37]. Magnetic micro-discs are capable of not only disrupting the integrity of a cell membrane, but also of triggering the apoptosis of cancer cells *in vitro* as a result of exposure to LFMF with a frequency of several tens of hertz for 10,min [38]. *in vivo*, cancer cell apoptosis is achieved through the use of spherical MNP by targeting the DR4 receptor [39]. It was shown that it is possible to control the expression of a ligand protein bound to cubic superparamagnetic iron oxide nanoparticles under a 30-minute exposure to LFMF with a frequency of 50 Hz [40]. In addition, recent studies have demonstrated the possibility of controlling enzyme activity using pulse modes of LFMF (1 s/0.3 s and 1 min/30 s pulse/pause duration, respectively) [41,42].

In a number of studies, it has been directly shown that the effect of LFMF on MNP does not lead to significant heating of the medium [43,44]. The activity of enzymes immobilized on MNP does not decrease under the influence of LFMF [41], the viability of cells with internalized magnetically sensitive capsules does not decline [43]. These experimental data indicate the fact that the use of magnetomechanical actuation is quite compatible with biological systems.

However, the number of experimental studies remains quite small. The above theoretical studies where the features of MNP rotation behavior are examined, mainly consider the systems MNP −macromolecule−MNP. The purpose of this work is to analyze the rotation behavior of MNPs embedded in the shells of polyelectrolyte capsules using computer modeling, as well as to compare the shell deformations that can be achieved under the influence of continuous and pulsed magnetic fields. The deformations of polyelectrolyte shells were analyzed taking into account the typical parameters of nanoparticles used for their modification. Due to the developed synthesis methods, excellent biocompatibility, pronounced superparamagnetic properties and the ability to uniformly functionalize the capsule shell with them, MNP of iron oxides with a size of about 10

nm are the most commonly used. Such particles have a pronounced Brownian mechanism of magnetic moment relaxation, which, combined with other characteristics, can ensure predictable and controlled behavior of nanoparticles when exposed to magnetic fields.

2. Results of numerical modelling

2.1. Rotation of MNP in continuous LFMF

To describe the behavior of MNP motion in the PEC shell under the action of LFMF, consider the equation of rotation of a single spherical MNP [28,29]:

$$I\ddot{\varphi} = \boldsymbol{\mu} \times \mathbf{B}(t) - 8\pi\eta V_{HD}\dot{\varphi} - M \cdot (\varphi - \varphi_0), \qquad (1)$$

where I — moment of inertia of MNP, $\boldsymbol{\mu}$ — vector of magnetic moment of MNP, $\mathbf{B}(t)$ — induction vector of magnetic field, η — viscosity in MNP micro-environment, V_{HD} — hydrodynamic volume of MNP, φ — current angle of MNP rotation, φ_0 — initial angle of MNP rotation, $M \cdot (\varphi - \varphi_0)$ — moment of elastic forces acting from the shell when MNP rotates at an angle of $(\varphi - \varphi_0)$.

For modeling let's reduce the equation (1) to the form:

$$\ddot{\varphi} + b\dot{\varphi} + c \cdot (\varphi - \varphi_0) = d^* \sin(\omega t)\cos(\varphi), \qquad (2)$$

where ω — frequency of LFMF, b — $8\pi\eta V_{HD}/I$, c — M/I, d — $\mu \cdot B/I$.

This equation was solved numerically at various values of parameter c and fixed values $b = 1$, $d = 1$. A resonance of MNP rotation is observed in the system, i.e., an increase in the amplitude of rotation. Depending on the elastic parameters of the system (parameter c in equation (2)), the amplitude and frequency of the resonance may change their values. Higher shell stiffness, i.e., increase of c, leads to higher resonant frequency of the PEC shell and lower resonance amplitude, which is demonstrated in Fig. 1.

Assuming that we have linear dependence of permeability of the shell for the encapsulated substance on the amplitude of rotation, we may talk about presence of a resonance enhancement in the permeability of PEC shell deformation. The resonant amplification of the release associated with the mechanical deformation of the PEC shell has previously been shown experimentally [26,45].

2.2. Rotation of MNP in pulsed LFMF

For the reviewed MNP system in PEC shells, the effect of pulsed fields with a sinusoidal pulse shape is of great interest. During the pauses between the pulses, the magnitude of magnetic field induction was assumed to be zero. At the beginning of each pulse, the parameters of magnetic field corresponded to the parameters of magnetic field at the initial time. During the pauses between pulses, the PEC shell relaxes into an undeformed state. Two different situations may occur:

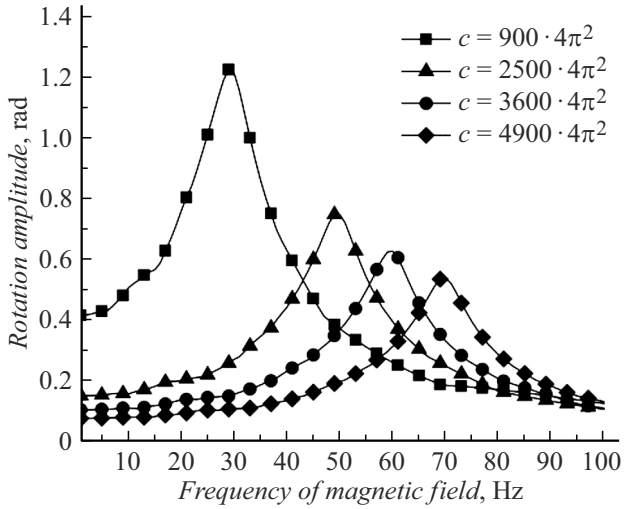

Figure 1. The dependence of the amplitude of MNP rotation in the PEC shell on the frequency of LFMF at different values of parameter c (the rest of the parameters remain constant).

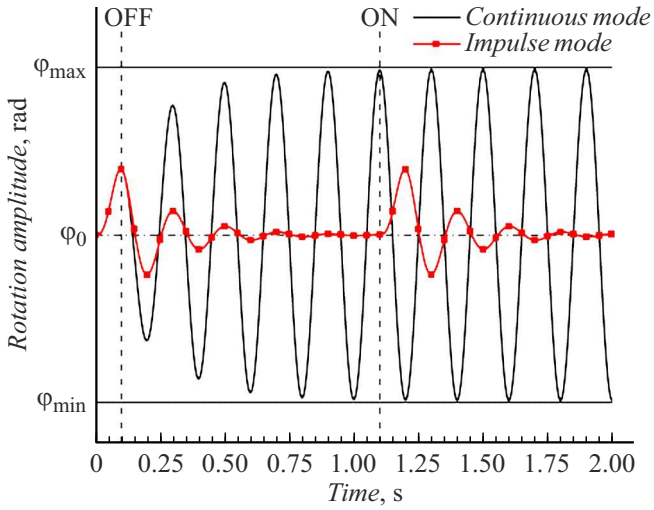

Figure 2. The angle of rotation of MNP in PEC shell under the influence of continuous and pulsed permanent magnetic field (the duration of pause between the pulses is longer than the duration of shell relaxation) ($T_{imp} = 0.1$ s, $T_{pause} = 1.0$ s).

1. The time of pause is higher than the shell relaxation time. In this case the shell is relaxed to the non-deformed state. The relaxation time depends on elastic properties of the shell and viscosity inside the shell (parameters b and c in equation (2) respectively). Due to the action of inertial forces, relaxation has an oscillating form. Figure 2 shows the time dependence of MNP rotation angle under continuous and pulsed exposure to LFMF with a frequency of 5 Hz (the resonant shell frequency of 5 Hz was used for modeling in both modes). Vertical lines show LFMF switching OFF and ON for the pulse mode.

2. The time of pause is less than the shell relaxation time. The shell has no enough time to relax. In this case,

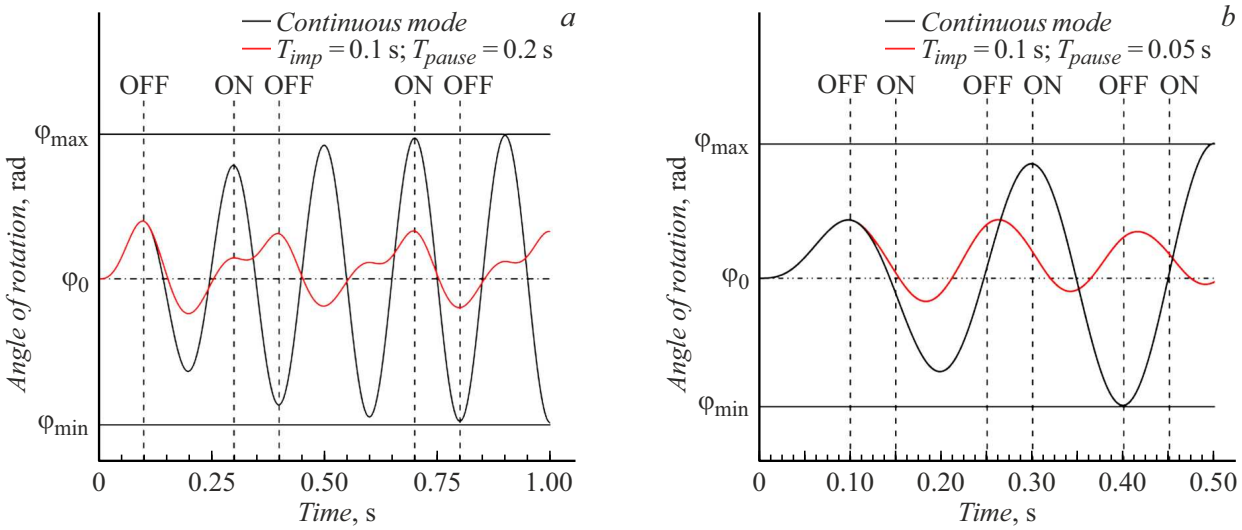

Figure 3. The angle of rotation of MNP in PEC shell under the influence of continuous and pulsed permanent magnetic field (the duration of pause between the pulses is less than the duration of shell relaxation) :*a* — $T_{imp} = 0.1$ s, $T_{pause} = 0.2$ s, *b* — $T_{imp} = 0.1$ s, $T_{pause} = 0.05$ s.

the dependence of the rotation angle on time may have a rather complex relationship as illustrated in Fig. 3. For modeling, LFMP with a frequency of 5 Hz and a resonant shell frequency of 5 Hz were used for both modes. Vertical lines show the moments of LFMF switching OFF and ON for the impulse modes.

As can be seen from Fig. 3 the decrease in duration of pause lead to less time for the shell to relax. At the moment of the next activation of magnetic field, MNP begins to experience its effects.

To compare the impulse and continuous modes of exposure to LFMF, we introduce a time-averaged rotation angle modulus ($\langle\Delta\varphi\rangle_t$) MNP PEC shell:

$$\langle\Delta\varphi\rangle_t = \frac{1}{t_{act}} \int_0^{t_{act}} |\Delta\varphi(t)|dt, \qquad (3)$$

where $\Delta\varphi(t)$ — deviation of MNP at a moment of time t from initial position, t_{act} — general exposure time.

This value characterizes the time-average deviation of MNP from the equilibrium position. Let's assume that $\langle\Delta\varphi\rangle_t$ and variation of PEC permeability have linear dependence. Then exposure to LFMF with modes for which $\langle\Delta\varphi\rangle_t$ is higher will lead to a greater release of encapsulated substances.

Figure 4 shows the maximum normalized dependence $\langle\Delta\varphi\rangle_t$ on the frequency of LFMP and the resonant frequency of PEC shell under continuous exposure. The obtained dependence is similar to that given in Figure 1. The highest value $\langle\Delta\varphi\rangle_t$ is achieved in the low-frequency region when the resonant frequency for PEC shell and the frequency of LFMP coincide. When the frequency of LFMP differs from the resonant frequency of the shell, the value of $\langle\Delta\varphi\rangle_t$ decreases rapidly and becomes smaller by a factor of 10^2-10^3 times. It can be seen from Fig. 4 that when the frequency of LFMP and the resonant frequency of the shell $\langle\Delta\varphi\rangle_t$ coincide, it decreases tenfold with the frequencies rising from 10 to 100Hz.

Impulse modes compared to continuous modes can lead to an increase or decrease in $\langle\Delta\varphi\rangle_t$ depending on the pulse duration, pause time, frequency of magnetic field and elastic characteristics of the system itself.

Figure 5 shows the values $\langle\Delta\varphi\rangle_t$ for impulse modes, normalized to the maximum value. For each pair of values of the PEC shell's resonant frequency and LFMF frequency, PEC rotation in the PEC shell was simulated at different LFMP pulse and pause durations (T_{imp} and T_{pause} within 0−1 s, step — 0.005 s). Based on the modeling results, an impulse mode with the highest value $\langle\Delta\varphi\rangle_t$ was selected for each pair of values of the PEC shell resonant frequency and LFMP frequency.

The dependences of $\langle\Delta\varphi\rangle_t$ on the frequency of the magnetic field and resonant frequency for PEC shell in continuous (Fig. 4) and pulsed (Fig. 5) modes of exposure to low-frequency magnetic radiation have similar nature, however, in case of pulsed modes, when the frequency of the magnetic field and the resonant frequency of the PEC shell do not match, the decrease $\langle\Delta\varphi\rangle_t$ occurs more smoothly than in the case of continuous exposure mode.

To evaluate the effectiveness of impulse modes versus continuous modes, the ratio of the largest $\langle\Delta\varphi\rangle_{t\_imp}$ impulse mode to $\langle\Delta\varphi\rangle_{t\_cont}$ of continuous mode was obtained for each pair of magnetic field frequency and resonant frequency values for the PEC shell. Fig. 6 illustrates a heat map $\langle\Delta\varphi\rangle_{t\_imp}/\langle\Delta\varphi\rangle_{t\_cont}$.

Figure 6 shows that on the diagonal, which corresponds to the close values of the magnetic field frequency and the resonant frequency of PEC shell, $\langle\Delta\varphi\rangle_{t\_imp} \sim \langle\Delta\varphi\rangle_{t\_cont}$.

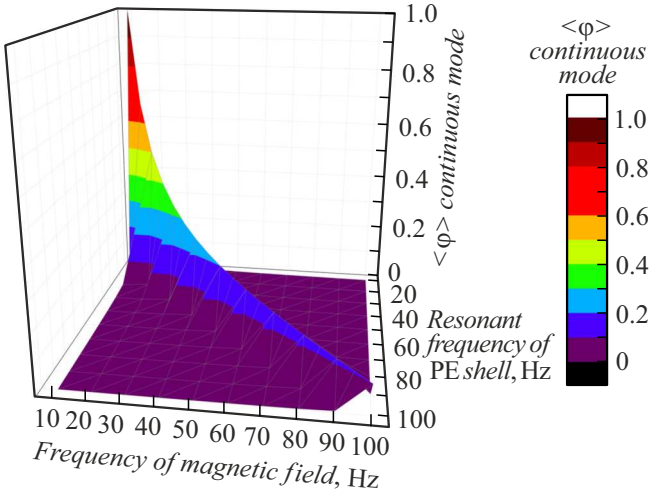

Figure 4. The values of the time-averaged deformation under continuous action of LFMF of different frequencies on PEC with different resonant shell frequencies.

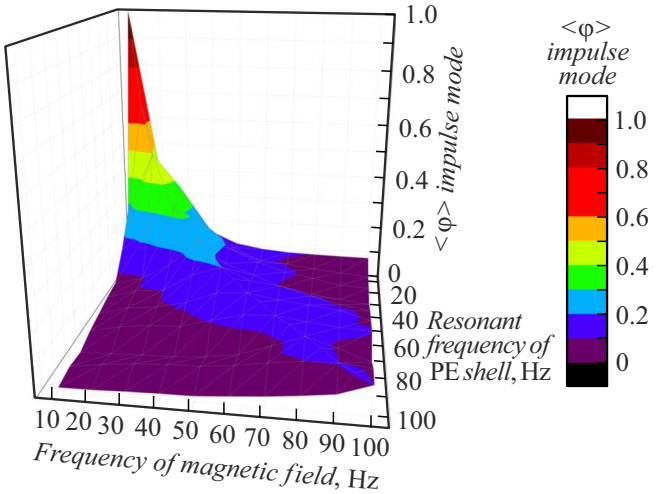

Figure 5. The values of the maximal time-averaged deformation under continuous impulse action of LFMF of different frequencies on PEC with different resonant shell frequencies.

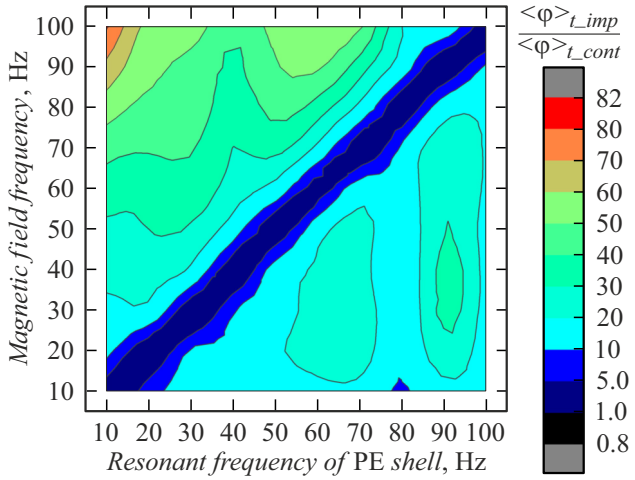

Figure 6. Heat map of the ratio of the largest $\langle\Delta\varphi\rangle_{t\_imp}$ impulse mode to $\langle\Delta\varphi\rangle_{t\_cont}$ continuous mode for different values of the frequency of LFMF and the resonant frequency of PEC shell.

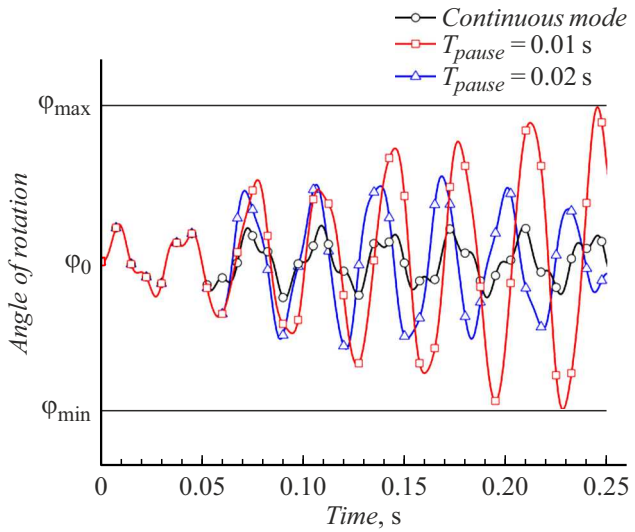

Figure 7. Orientation of MNP in the PEC shell exposed to LFMF in continuous and impulse modes ($T_{imp} = 0.05$ s) when $\langle\Delta\varphi\rangle_t$ is increased in many times.

In this frequency range, the deformations created during continuous and impulse modes differ by no more than 5 times. This is due to the presence of pauses in impulse modes, during which the shell relaxes into an non-deformed state. In this regard, in this field it is difficult to figure out the preferred mode of exposure in which deformations would be greatest.

In the regions of significant difference between the frequencies of magnetic field and the resonant frequencies of PEC shells, deformations occur in impulse modes that exceed deformations under continuous action of LFMF by tens of times. The greatest differences are observed when the frequency of LFMP exceeds the resonant frequency of the PEC shell (the area above the diagonal in Fig. 6). Let's consider this region in the map in details, having selected the values of LFMF frequency and resonant frequency of PEC shell as 80 and 30 Hz, respectively.

Fig. 7 shows dependence $\varphi(t)$ for continuous and several impulse modes in case when frequencies do not coincide (LFMF frequency — 80 Hz, resonant frequency of the PEC shell — 30 Hz). The dependence demonstrates how the orientation of the particles' magnetic moment in the shell changes over time.

The curve corresponding to continuous mode intersects the straight line φ_0 more times than all the curves corresponding to the impulse modes. Besides, the values of rotation amplitudes for continuous mode are lower than for impulse ones (regardless of the duration of pauses). This results in higher $\langle\Delta\varphi\rangle_t$ in case of impulse mode.

3. Discussion

The above results were obtained for different values of parameter c and fixed values $b = 1$, $d = 1$, of equation (2). Papers [28,29] give the following estimates of parameters b and d: $d \sim 10^{14}-10^{17}$, $b \sim 10^{11}-10^{12}$. The estimated values of parameter c can be obtained based on the values of Young's modulus for polyelectrolyte capsules from papers [46,47]. Summarizing the results of these two papers, we can conclude that for polyelectrolyte capsules, the value of Young's modulus is $E \sim 1-100$ MPa. Then the value of parameter c for polyelectrolyte capsules can be estimated as

$$c \sim \frac{RE\frac{S}{L}}{\rho R^5} \approx 10^{28}-10^{30}, \quad (4)$$

where R — the radius of magnetic nanoparticles, E — Young's modulus, L — length of the part of the polymer matrix deformed by rotation of the magnetic nanoparticle, S — cross-sectional area of the polymer matrix portion deformed by rotation of the magnetic nanoparticle, ρ — density of the MNP material. In the obtained estimate the following values were used$L \sim 10^{-8}$ m, $R \sim 10^{-8}$ m, $S \sim 10^{-16}$ m^2, $\rho \sim 5 \cdot 10^3$ kg/m^3. The value for L was based on the estimate of the polyelectrolyte chain length with the polyelectrolyte mass of 50−100 kDa [48,49]. With such a polyelectrolyte mass, the length of the polyelectrolyte chain is 10−20 nm.

Based on theoretical concepts of [50], if we have values $b \sim 10^{14}-10^{15}$ and $c \sim 10^{28}-10^{30}$, it is possible to obtain the resonant frequency of the polyelectrolyte shell up to 100Hz.

It is worth noting that large values of the parameters b and c lead to a decrease in the magnitude of the resonant peak, and, hence, to a decrease in the efficiency of the release of encapsulated substances when exposed to LFMF. Despite this, the existing experimental results on the release of fluorescent-labeled dextran, bovine serum albumin, mitoxantrone, and doxycycline [25,26,43,45] from polyelectrolyte capsules prove that it is possible to use continuous LFMF for a controlled impact on permeability of their shells.

Conclusion

In this paper, the behavior pattern of MNP rotation in the PEC shell under the influence of LFMF is analyzed. The MNP rotation in the PEC shell was modelled at different LFMF parameters.

1. It was proved by computer modeling that MNP rotates in the shell with a resonant frequency. Previously, the resonant frequency of MNP rotation assumed was based on experimental data.

2. It was demonstrated that in case of close values of the field's and the PEC shell's frequencies, the impulse and continuous modes of LFMF allow the commensurable deformations to occur.

3. In case of impulse action of LFMF with a frequency different from the resonant (natural) frequency of the PEC shell, it is possible to increase deformation of the PEC shell (and hence its permeability) several times compared to continuous action of LFMF. The greatest effect is achieved when LFMF frequencies outpace the resonant frequency of the PEC shell.

Funding

This study was carried out under the state assignment of National Research Center „Kurchatov Institute."

Conflict of interest

The authors declare that they have no conflict of interest.

References

[1] M. Lengyel, N. Kállai-Szabó, V. Antal, A.J. Laki, I. Antal. Scientia Pharmaceutica, **87** (3), 20 (2019). DOI: 10.3390/scipharm87030020
[2] A. Tewabe, A. Abate, M. Tamrie, A. Seyfu, E.A. Siraj. J. Multidisciplinary Healthcare, **14**, 1711 (2021). DOI: 10.2147/JMDH.S313968
[3] F.M. Kashkooli, M. Soltani, M. Souri. J. Controlled Release, **327**, 316 (2020). DOI: 10.1016/j.jconrel.2020.08.012
[4] A.S. Timin, D.J. Gould, G.B. Sukhorukov. Expert Opinion on Drug Delivery, **14** (5), 583 (2017). DOI: 10.1080/17425247.2017.1285279
[5] R. Kurapati, T.W. Groth, A.M. Raichur. ACS Appl. Bio Mater., **2** (12), 5512 (2019). DOI: 10.1021/acsabm.9b00703
[6] H. Zhang, Q. Wang, Y. Li, Y. Zhao. Gels, **8** (9), 583 (2022). DOI: 10.3390/gels8090583
[7] Y. Liu, Ch. Liu, J. Liu, Y. Qiao, Y. Liu, Y. Zhou, G. Li, Z. Yang, Z. Lia, Z. Sun. New J. Chem., **47** (1), 46 (2023).
[8] J. Fan, M. Xuan, P. Zhao, M. Loznik, J. Chen, F. Kiessling, L. Zheng, A. Herrmann. Nano Research, **16** (2), 2738 (2023). DOI: 10.1007/s12274-022-4919-9
[9] D.A. Gorin, S.A. Portnov, O.A. Inozemtseva, Z. Luklinska, A.M. Yashchenok, A.M. Pavlov, A.G. Skirtach, H. Möhwald, G.B. Sukhorukov. Phys. Chem. Chem. Phys., **10** (45), 6899 (2008).
[10] I. Burmistrov, M. Veselov, A. Mikheev, T. Pallaeva, T.V. Bukreeva, N. Klyachko, D. Trushina. Med. Sci. Forum, **14** (1), 90 (2022). DOI: 10.3390/ECMC2022-13495
[11] E.S. Vavaev, M. Novoselova, N.M. Shchelkunov, S. German, A.S. Komlev, M.D. Mokrousov, I.V. Zelepukin, A.M. Burov, B.N. Khlebtsov, E.V. Lyubin, S. Deyev, A.A. Fedyanin, D.A. Gorin. ACS Appl. Nano Mater., **5** (2), 2994 (2022). DOI: 10.1021/acsanm.2c00338
[12] J. Gao, J.M. Karp, R. Langer, N. Joshi. Chem. Mater., **35** (2), 359 (2023). DOI: 10.1021/acs.chemmater.2c03003
[13] N.M. AlSawaftah, N.S. Awad, W.G. Pitt, G.A. Husseini. Polymers, **14** (5), 936 (2022). DOI: 10.3390/polym14050936
[14] D.K. Kim, J. Dobson. J. Mater. Chem., **19** (35), 6294 (2009). DOI: 10.1039/B902711B
[15] A.P. Esser-Kahn, S.A. Odom, N.R. Sottos, S.R. White, J.S. Moore. Macromolecules, **44** (14), 5539 (2011). DOI: 10.1021/ma201014n

[16] S.U. Ahmad, B. Li, J. Sun, S. Arbab, Z. Dong, F. Cheng, X. Zhou, S. Mahfuz, J. Zhang. J. Veterinary Pharmacology and Therapeutics, **44** (3), 298 (2021). DOI: 10.1111/jvp.12946
[17] L.-Y. Chu, S.-H. Park, T. Yamaguchi, Sh.-ichi Nakao. Langmuir, **18** (5), 1856 (2002). DOI: 10.1021/la011385h
[18] X. Feng, Y. Zhu, Zh. Liu, C. Meng, L. Yang, X. Han, J. Yang, X. Jia. ACS Agricultural Sci. Technol., **1** (5), 507 (2021). DOI: 10.1021/acsagscitech.1c00122
[19] Y.H. Choi, J.-S. Hwang, S.H. Han, Ch.-S. Lee, S.-J. Jeon, Sh.-H. Kim. Adv. Functional Mater., **31** (24), 2100782 (2021).
[20] R. Klitzing, H. Möhwald. Macromolecules, **29** (21), 6901 (1996). DOI: 10.1021/MA960240S
[21] A. Kikuchi, M. Kawabuchi, A. Watanabe, M. Sugihara, Y. Sakurai, T. Okano. J. Controlled Release, **58** (1), 21 (1999). DOI: 10.1016/s0168-3659(98)00141-2
[22] F. He, li Mei, X.-J. Ju, R. Xie, W. Wang, Zh. Liu, F. Wu, L.-Y. Chu. J. Membrane Sci., **474**, 233 (2015). DOI: 10.1016/j.memsci.2014.10.012
[23] M.N. Singh, K.S.Y. Hemant, M. Ram, H.G. Shivakumar. Research in Pharmaceutical Sci., **5** (2), 65 (2010).
[24] Z. Lu, M.D. Prouty, Zh. Guo, V.O. Golub, Ch.S.S.R. Kumar, Yu.M. Lvov. Langmuir, **21** (5), 2042 (2005). DOI: 10.1021/la047629q
[25] D. Luo, R.N. Poston, D.J. Gould, G.B. Sukhorukov. Materials Science and Engineering: C, **94**, 647 (2019).
[26] I.A. Burmistrov, M.M. Veselov, A.V. Mikheev, T.N. Borodina, T.V. Bukreeva, M.A. Chuev, S.S. Starchikov, I.S. Lyubutin, V.V. Artemov, D.N. Khmelenin, N.L. Klyachko, D.B. Trushina. Pharmaceutics, **14** (1), 65 (2021). DOI: 10.3390/pharmaceutics14010065
[27] K. Wu, K. Schliep, X. Zhang, J. Liu, B. Ma, J.-P. Wang. Small, **13** (22), 1604135 (2017). DOI: 10.1002/smll.201770124
[28] Yu.I. Golovin, S.L. Gribanovsky, N.L. Klyachko, A.V. Kabanov. ZhTF, **84** (6), 147 (2014) (in Russian).
[29] Yu.I. Golovin, S.L. Gribanovsky, D.Yu. Golovin, N.L. Klyachko, A.V. Kabanov. FTT, **56** (7), 1292 (2014). (in Russian)
[30] A.A. Nikitin, A.V. Ivanova, A.S. Semkina, P.A. Lazareva, M.A. Abakumov. Int. J. Mol. Sci., **23**, 11134 (2022). DOI: 10.3390/ijms231911134
[31] Yu.I. Golovin, N.L. Klyachko, S.L. Gribanovskii, D.Yu. Golovin, A.A. Samodurov, A.G. Majouga, M. Sokolsky-Papkov, A.V. Kabanov. Tech. Phys. Lett., **41**, 455 (2015).
[32] C. Naud, C. Thébault, M. Carrière, Y. Hou, R. Morel, F. Berger, B. Diény, H. Joisten. Nanoscale Adv., **2** (9), 3632 (2020). DOI: 10.1039/D0NA00187B
[33] K.Yu. Vlasova, H. Vishwasrao, M.A. Abakumov, D.Yu. Golovin, S.L. Gribanovsky, A.O. Zhigachev, A.A. Poloznikov, A.G. Majouga, Yu.I. Golovin, M. Sokolsky-Papkov, N.L. Klyachko, A.V. Kabanov. Scientific Reports, **10** (1), 4745 (2020). DOI: 10.1038/s41598-020-61364-w
[34] A.R. Iliasov, T. Nizamov, V.A. Naumenko, A. Garanina, S. Vodopyanov, A. Nikitin, A.G. Pershina, A.A. Chernysheva, Y. Kan, P.S. Mogilnikov, O. Metelkina, I.V. Schetinin, A. Savchenko, A.G. Majouga, M.A. Abakumov. Colloids and Surfaces B: Biointerfaces, **206**, 111931 (2021). DOI: 10.1016/j.colsurfb.2021.111931
[35] A.A. Nikitin, A.Yu. Yurenya, T.S. Zatsepin, I.O. Aparin, V.P. Chekhonin, A.G. Majouga, M. Farle, U. Wiedwald, M.A. Abakumov. ACS Appl. Mater. Interfaces, **13** (12), 14458 (2021). DOI: 10.1021/acsami.0c21002
[36] S. Lopez, N. Hallali, Y. Lalatonne, A. Hillion, J.C. Antunes, N. Serhan, P. Clerc, D. Fourmy, L. Motte, J. Carrey, V. Gigoux. Nanoscale Adv., **4** (2), 421 (2022). DOI: 10.1039/D1NA00474C
[37] S. Yun, T.-H. Shin, J.-H. Lee, M.H. Cho, Il-S. Kim, Ji-w. Kim, K. Jung, Il-Sh. Lee, J. Cheon, K. In Park. Nano Lett., **18** (2), 838 (2018). DOI: 10.1021/acs.nanolett.7b04089
[38] D.-H. Kim, E.A. Rozhkova, I.V. Ulasov, S.D. Bader, T. Rajh, M.S. Lesniak, V. Novosad. Nature Mater., **9** (2), 165 (2010). DOI: 10.1038/nmat2591
[39] M.H. Cho, E.J. Lee, M. Son, J.-H. Lee, D. Yoo, J.-Wook Kim, S.W. Park, J.-S. Shin, J. Cheon. Nature Mater., **11** (12), 1038 (2012). DOI: 10.1038/nmat3430
[40] J. Beltran-Huarac, D.N. Yamaleyeva, G. Dotti, Sh. Hingtgen, M. Sokolsky-Papkov, A.V. Kabanov. ACS Appl. Mater. Interfaces, **15** (16), 19877 (2023). DOI: 10.1021/acsami.3c00179
[41] A.D. Usvaliev, N.G. Belogurova, K.V. Pokholok, A.V. Finko, A.N. Prusov, D.Yu. Golovin, K.A. Miroshnikov, Yu.I. Golovin, N.L. Klyachko. Pharmaceutics, **15** (7), 1871 (2023). DOI: 10.3390/pharmaceutics15071871
[42] M. Veselov, M.V. Efremova, A.N. Prusov, N. Klyachko. Nanomaterials, **14** (5), 411 (2024). DOI: 10.3390/nano14050411
[43] A.A. Abalymov, R.A. Anisimov, P.A. Demina, V.A. Kildisheva, A.E. Kalinova, A.A. Serdobintsev, N.G. Novikova, D.B. Petrenko, A.V. Sadovnikov, D.V. Voronin, M.V. Lomova. Biomedicines, **12** (2), 443 (2024). DOI: 10.3390/biomedicines12020443
[44] I.M. Le-Deygen, K.Yu. Vlasova, E.O. Kutsenok, A.D. Usvaliev, M.V. Efremova, A.O. Zhigachev, P.G. Rudakovskaya, D.Yu. Golovin, S.L. Gribanovsky, E.V. Kudryashova, A.G. Majouga, Yu.I. Golovin, A.V. Kabanov, N.L. Klyachko. Nanomedicine, **21**, 102065 (2019).
[45] A. Mikheev, I. Burmistrov, V.B. Zaytsev, V.V. Artemov, D. Khmelenin, S.S. Starchikov, M. Veselov, N. Klyachko, T.V. Bukreeva, D. Trushina. J. Surf. Investigation: X-Ray, Synchrotron and Neutron Techniques, **16** (1), 7 (2022). DOI: 10.1134/S1027451021060355
[46] V.V. Lulevich, D. Andrienko, O.I. Vinogradova. J. Chem. Phys., **120** (8), 3822 (2004). DOI: 10.1063/1.1644104
[47] O.I. Vinogradova, D. Andrienko, V.V. Lulevich, S. Nordschild, G.B. Sukhorukov. Macromolecules, **37** (3), 1113 (2004). DOI: 10.1021/ma0350213
[48] B. Jachimska, T. Jasiński, P. Warszyński, Z. Adamczyk. Colloids and Surfaces A: Physicochemical and Engineering Aspects, **355** (1−3), 2010, 7 (2010). DOI: 10.1016/j.colsurfa.2009.11.012
[49] A. Han, R.H. Colby. Macromolecules, **54** (3), 1375 (2021). DOI: 10.1021/acs.macromol.0c02437
[50] M.I.Rabinovich, D.I.Trubetskov. *Vvedeniye v teoriyu kolebaniy i voln* (Nauka, M., 1984) (in Russian).

Translated by T.Zorina